Prepared for submission to JHEP SLAC-PUB-16518

Solving the Wrong Hierarchy Problem

Nikita Blinov,[a] **Anson Hook**[b]

[a] *SLAC National Accelerator Laboratory, 2575 Sand Hill Road, Menlo Park, CA, 94025, USA*
[b] *Stanford Institute for Theoretical Physics, Stanford University, Stanford, CA 94305, USA*

E-mail: nblinov@slac.stanford.edu, hook@stanford.edu

Abstract: Many theories require augmenting the Standard Model with additional scalar fields with large order one couplings. We present a new solution to the hierarchy problem for these scalar fields. We explore parity- and $\mathbb{Z}_2$-symmetric theories where the Standard Model Higgs potential has two vacua. The parity or $\mathbb{Z}_2$ copy of the Higgs lives in the minimum far from the origin while our Higgs occupies the minimum near the origin of the potential. This approach results in a theory with multiple light scalar fields but with only a single hierarchy problem, since the bare mass is tied to the Higgs mass by a discrete symmetry. The new scalar does not have a new hierarchy problem associated with it because its expectation value and mass are generated by dimensional transmutation of the scalar quartic coupling. The location of the second Higgs minimum is not a free parameter, but is rather a function of the matter content of the theory. As a result, these theories are extremely predictive. We develop this idea in the context of a solution to the strong CP problem. We show this mechanism postdicts the top Yukawa to be within 1σ of the currently measured value and predicts scalar color octets with masses in the range 9-200 TeV.

arXiv:1605.03178v2 [hep-ph] 30 Jun 2016

Contents

1 Introduction **1**

2 Hierarchies and the Strong CP Problem **3**
- 2.1 A Predictive η' Solution to the Strong CP Problem 3
- 2.2 Cosmology with a Mirror Sector 7

3 Dimensional Transmutation from the Higgs quartic **7**
- 3.1 Tree-Level Potential in the $\mathbb{Z}_2$-symmetric Standard Model 8
- 3.2 Renormalization Group and the Effective Potential 8
- 3.3 Bifundamental Mass Scale 9

4 Conclusion **13**

A Integrating Through a Strongly Coupled Threshold **14**

B Higher Dimensional Operators in the Scalar Potential **16**

1 Introduction

The Standard Model (SM) Higgs boson mass is sensitive to ultraviolet (UV) physics. This is the hierarchy problem. Traditional solutions to the hierarchy problem have postulated the existence of new particles that appear at low scales to cancel the quadratic dependence on UV physics. Recently there has been renewed focus on non-traditional solutions to the hierarchy problem, such as the multiverse, the relaxion [1], and NNaturalness [2]. In these solutions, the Higgs mass appears to have been fine tuned to be small.

Aside from the hierarchy problem, the SM has other issues that require explanations, such as the origin of flavor, baryogenesis and the strong CP problem. Solutions to these problems often introduce new heavy scalar degrees of freedom. These scalar fields also suffer from quadratic sensitivity to UV physics. Usually these "wrong" hierarchy problems are resolved in the same way as the electroweak hierarchy. In this work, we present a new solution to this secondary hierarchy problem that operates when the naturalness of the electroweak scale is explained using one of the non-traditional mechanisms mentioned above.

Our approach employs dimensional transmutation through the Coleman-Weinberg mechanism to dynamically generate a new hierarchy of scales [3]. Standard use of dimensional transmutation to stabilize scalar mass relies on gauge couplings becoming strong and gives rise to the large separation between the QCD and the electroweak scales. When applied to the usual naturalness problem, it leads to technicolor and its variants. There is another

kind of dimensional transmutation which occurs in the SM and involves the Higgs scalar quartic instead of a gauge coupling. This effect is well known through the renormalization group evolution (RGE) of the Higgs self-coupling λ, which generates a maximum in the Higgs potential and an instability at large field values [4–6]. The dimensional transmutation aspect of this mechanism was emphasized in Ref. [7]. We utilize this effect to solve the secondary hierarchy problem discussed above. A similar approach was used to dynamically generate the Planck scale in Ref. [8].

Our Higgs field occupies the very long lived electroweak minimum, so the apparent run-away of the potential at large field values h is irrelevant. However, in parity- or $\mathbb{Z}_2$-symmetric theories, there is a second Higgs with a similar potential. Additional matter can radiatively stabilize this potential at large h and generate a second minimum that is much deeper than the electroweak one. If the second Higgs occupies this true vacuum, it can provide a new heavy scale that can be used to solve any of the aforementioned problems. This new scale is generated by dimensional transmutation and so there is no new hierarchy problem.

In order for the dimensional transmutation of the scalar quartic to be important, the relevant mass term must be small. We use a discrete symmetry to link this new scalar mass with the Higgs mass. In this way, the mechanism that solves the standard hierarchy problem also ensures the mass parameter of the new scalar field remains small. Thus our starting point is a $\mathbb{Z}_2$ or parity symmetric theory, where the symmetry operation exchanges SM fields for their "mirror" partners.[1] The discrete symmetry guarantees that the renormalization group running of couplings in the mirror sector is identical to the SM at high scales. This ensures that the potential for the $\mathbb{Z}_2$ partner of the Higgs H' can be determined by studying the potential of the SM Higgs boson H.

The tree-level $\mathbb{Z}_2$ symmetric scalar potential has several minima. These minima have many problems. There are new light particles and the new scalar is at the weak scale or lower, making it too light for the solution of, e.g., flavor or strong CP problems. Thus it is impossible to get a hierarchy between $h = \sqrt{2}\langle H\rangle$ and $h' = \sqrt{2}\langle H'\rangle$ at *tree-level*. Renormalization group evolution is necessary for h' to be separated from the weak scale. Because logarithmic RGE requires a large amount of running to be effective, this new scale will be parametrically larger than the weak scale.

There is a simple way to obtain the large amount of running needed to generate a new scale. If the masses of the scalars are parametrically below the cutoff Λ, then loop corrections to the effective potential may create a new minimum where $\Lambda \gg h' \gg h$. In order for the mass term m_H to not be important in determining the location of the minimum, we necessarily have $h' \gg m_H$.[2]

Because all of the SM parameters have been measured, the location of the second vacuum is determined by the matter content of the theory. Thus the new heavy scale is

[1] Similar $\mathbb{Z}_2$-symmetric constructions have been used, for example, to explain dark matter and the baryon asymmetry of the universe, naturalness of the weak scale and to solve the strong CP problem – see Refs. [9–15] and references therein.

[2] Another way for RG running of the Higgs quartic to play a role is in tuned Twin Higgs models [10]. As it is similar to what we consider here, we leave this example as an exercise for the reader.

completely determined without the introduction of new dimensionful parameters, leading to a very predictive framework. The radiatively generated scale is most sensitive to the strong coupling α_s and top quark Yukawa y_t. Precise measurements of these quantities will be necessary to accurately determine the new energy scale.

In this work we illustrate this mechanism by considering an η' solution to the strong CP problem [13]. A $\mathbb{Z}_2$ symmetry and new massless quarks allow the QCD θ angle to be rotated away. Dimensional transmutation naturally determines the vacuum expectation value (vev) of the $\mathbb{Z}_2$ Higgs copy to be below the Planck scale, fixes the masses of colored states (originating from the new quarks) and precisely predicts the top quark Yukawa to be within 1σ of the currently measured value.

This paper is organized as follows. In Sec. 2.1, we present a solution to the wrong hierarchy problem in the context of an η' explanation of the strong CP problem finding interesting experimental predictions. In Sec. 3 we discuss the details of the Higgs potential in this solution to the strong CP problem. We briefly consider further applications of this mechanism and conclude in Sec. 4. Technical details are collected in the Appendices.

2 Hierarchies and the Strong CP Problem

In this section, we illustrate our solution to the wrong hierarchy problem in the context of a predictive η' explanation of the strong CP problem. Discrete symmetry-based solutions of strong CP involve a new scale where this symmetry is spontaneously broken. Stabilizing this new scale with traditional solutions such as supersymmetry (SUSY) is difficult due to the plethora of new phases introduced by SUSY breaking and due to unsuppressed renormalization group running of θ [16, 17]. In contrast, our solution does not introduce new CP violating phases and preserves the small running of θ present in the SM.

The minimal η' solution to the strong CP problem involves two copies of the SM related by a $\mathbb{Z}_2$ symmetry. In addition, there are new massless vector-like fermions, ψ and ψ^c, which are bifundamentals under our QCD and QCD$'$ (the $\mathbb{Z}_2$ copy of QCD).[3] In the absence of a vector-like mass, an anomalous $U(1)$ rotation of ψ and/or ψ^c is used to set the sum of the two theta angles to zero, while their difference is zero by the $\mathbb{Z}_2$ symmetry. Thus the strong CP problem is solved in the unbroken $\mathbb{Z}_2$ limit.

Non-observation of new light states suggests that $\mathbb{Z}_2$ breaking must occur and that the mirror sector's Higgs vev must be large, potentially introducing a new hierarchy problem. In our solution, the $\mathbb{Z}_2$ symmetry ensures that the tree-level mirror Higgs mass is small. As mentioned in the introduction, the $\mathbb{Z}_2$ breaking then comes from the RG running of the Higgs quartic so that the mirror Higgs obtains a large physical mass and vev without introducing a new hierarchy problem.

2.1 A Predictive η' Solution to the Strong CP Problem

As will be shown in the next section, the potential for each Higgs naturally contains two vacua in this scenario. If both Higgs bosons are in the same minimum, then the strong CP

[3] Mirror sector quantities are denoted with primes.

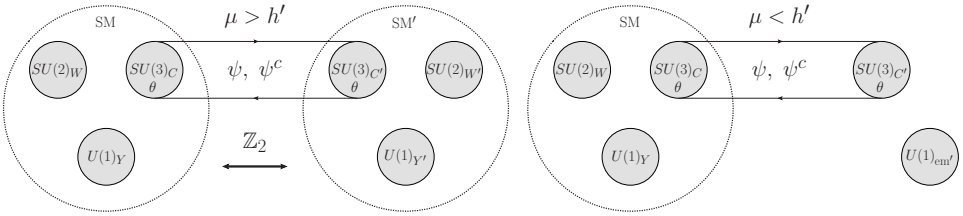

Figure 1: A pictorial representation of the η' solution to the strong CP problem at various RG scales μ. The left (right) diagram shows the model above (below) the $\mathbb{Z}_2$ breaking scale h'.

problem is solved by a chiral rotation of a massless quark. This solution is observationally excluded due to the presence of three new massless vector-like quarks. However, if the two Higgs bosons occupy different vacua, then the particles in the mirror sector can be much heavier than any SM states. Due to the larger h' vev, the quarks and leptons in the mirror sector are integrated out at much larger scales. After all of the new massive particles have been integrated out, the matter content is simply the SM augmented by the gauge group $SU(3)_{C'}$ and the associated bifundamentals ψ and ψ^c. At this point, because the $\mathbb{Z}_2$ symmetry has been broken by $h \neq h'$, the effective QCD angle $\overline{\theta}$ is reintroduced by renormalization group effects. However, as shown in Refs. [18, 19], the RG effects in these types of models are negligible. This model is shown schematically in Fig. 1 for RG scales $\mu \gg h'$ (left) and $\mu \ll h'$ (right).

After QCD′ confines, there are no more massless degrees of freedom in the infrared (IR) and the theory is simply the SM with extra massive colored states, the pseudo-Goldstone bosons of QCD′. As emphasized in Ref. [13], if the θ angle has not been rotated to zero, dynamic relaxation of the the η'' (the η' boson of QCD′) sets our $\overline{\theta}$ to zero. More explicitly, the IR effective theory of the η'' after QCD′ confines is

$$\mathscr{L} = \frac{g^2}{32\pi^2}\left(\overline{\theta} - \frac{\eta''}{f_{\eta''}}\right) G\tilde{G} + \frac{m_{\eta''}^2}{2}\left(\eta'' - f_{\eta''}\overline{\theta}'\right)^2 + \cdots \tag{2.1}$$

where the ellipsis stands for other terms in the chiral Lagrangian. Integrating out the η'' boson and using the $\mathbb{Z}_2$ symmetry ($\overline{\theta} = \overline{\theta}'$), we find that our theta angle has been set to zero.

The presence of ψ and ψ^c, three new flavors of $SU(3)_C$ quarks, introduces a small stabilizing effect on the RG running of the Higgs quartic and generates a second minimum in the Higgs potential for certain ranges of SM parameters. The location of this true minimum determines the confinement scale of QCD′ and therefore the mass scale of states associated with ψ and ψ^c. However, the scale where ψ and ψ^c are integrated in determines the true minimum. Therefore finding the true minimum is a recursive process that leads to somewhat counter-intuitive results. We leave a detailed discussion of the Higgs potential and the determination of the bifundamental mass scale to Sec. 3 and simply summarize the results here.

We find that the second minimum only exists for a small range of parameters. As the Higgs potential is most sensitive to the top quark Yukawa, we hold other parameters at their central measured values and vary the top quark mass M_t. The corresponding $\overline{\text{MS}}$ quantities also vary with M_t due to loop corrections [4–6]. The mirror Higgs vev as a function of M_t is shown in the left plot of Fig. 2. The determination of the uncertainty band is discussed in Sec. 3.3 and Appendix A. The top quark mass is postdicted to be in the range

$$172.4\,\text{GeV} < M_t < 173.2\,\text{GeV}. \tag{2.2}$$

This is to be compared with the measured value [20]

$$M_t = 173.34 \pm 0.87\,\text{GeV}. \tag{2.3}$$

The solution to the strong CP problem has accurately postdicted the top quark mass to within 1σ! Note that this postdiction depends on the representation of the $\psi^{(c)}$ states. Thus, precise measurements of M_t (such as those possible with the ILC [21]) can probe the UV content of this theory.

The small range of allowed top quark masses can be understood as follows. First, note that the smaller the radiatively-generated vev is, the earlier ψ and ψ^c are integrated into the RGEs and the larger their effect on the potential at high field values is. Therefore to counteract a larger y_t, ψ and ψ^c must appear sooner and thus the vev must decrease. This explains the negative slopes in the vev and the QCD$'$ confinement scale as a function of M_t shown in Fig. 2. Above the upper bound in Eq. 2.2, the bifundamentals are so light that their indirect effect is enough to completely stabilize the electroweak vacuum: the second minimum disappears. Below the lower bound in Eq. 2.2, the second Higgs minimum is pushed above the Planck scale. This can be understood by noting that for lower y_t the SM potential is nearly stable, so $\psi^{(c)}$ must be integrated in at a high scale. As y_t is lowered and the scale of $\psi^{(c)}$ is increased, the stabilization of the potential occurs at ever higher scales, eventually passing M_{Pl}. These arguments are made precise in the following section.

The lightest new particles in the theory come from the confinement of QCD$'$. Confinement is accompanied by the spontaneous breaking of global symmetry $SU(3)_L \times SU(3)_R \to SU(3)_D$, associated with the massless bifundamentals ψ and ψ^c (recall that *all* of the mirror quarks have been integrated out).[4] Analogously to QCD, the spectrum consists of an octet pseudo-Goldstone bosons π' and other mesons. The chiral symmetry is also explicitly broken by the gauging of QCD $SU(3)_C \subset SU(3)_L \times SU(3)_R$, so π' is a color octet. Thus, much like the charged pions, the π' obtain a mass from gluon loops. The confinement scale of QCD$'$ is determined by h'. Because $h' > h$, the mirror quarks are integrated out sooner and the confinement scale is larger than in QCD. The mass of the scalar color octet as a function of the top quark mass is shown in the right plot of Fig. 2. We find that these new particles are predicted to have a mass

$$9\,\text{TeV} < m_{\pi'} < 200\,\text{TeV}, \tag{2.4}$$

[4]The chiral symmetry breaking pattern depends on the representation of $\psi^{(c)}$. We work with bifundamentals of $SU(3)_C \times SU(3)_{C'}$ to make use of existing QCD results.

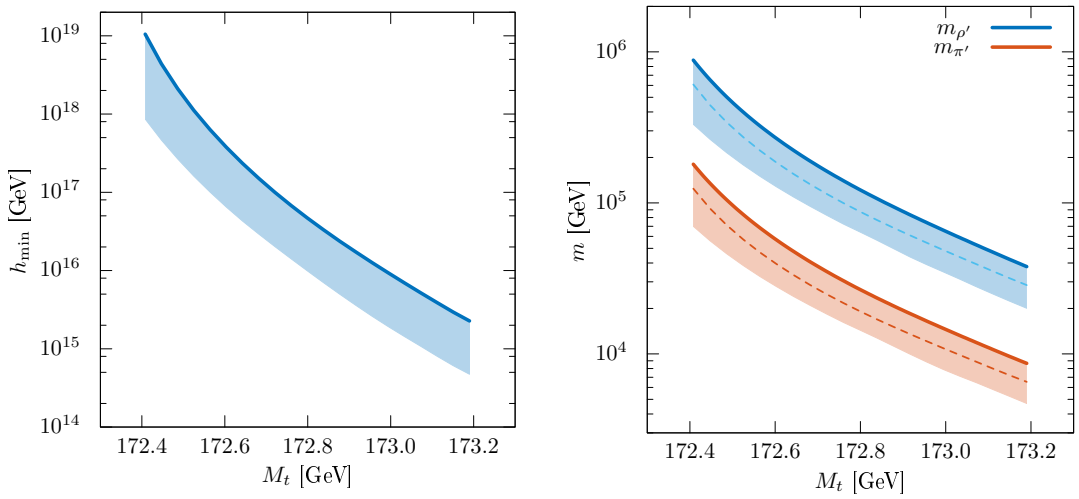

Figure 2: (Left) Dependence of the mirror Higgs VEV on the top quark mass M_t. (Right) The mass of the color octet ρ' (upper line) and π' mesons (lower line) as a function of M_t. The uncertainty bands shown are generated by varying the matching scale associated with running the QCD coupling through the strongly coupled regime of QCD$'$. The solid (dashed) line in each band corresponds to using the four (one) loop QCD$'$ beta function to determine the confinement scale $\Lambda_{\mathrm{QCD}'}$. Below the lower range of M_t shown the mirror Higgs vev moves above the Planck scale, while above the highest M_t shown no self-consistent solution for bifundamental mass scale exists.

where the range is set by the precise value of M_t. This new scalar color octet decays through the Wess-Zumino term into a pair of gluons, much like how the π^0 decays into a pair of photons. Single π' production can occur through the same interaction, leading to a resonant dijet signature at a hadron collider. While these states are too heavy to be produced at the LHC [22–24], a future 100 TeV collider will be able to probe a significant portion of this mass range [25]. We reserve the detailed study of collider signatures of this scenario to a future work.

Solutions to the strong CP problem are sensitive to UV physics through higher dimensional operators. These problems for axions [26] and the Nelson-Barr mechanism [17] are well known. In the present case, once $h \neq h'$, there is no symmetry protecting the QCD angle and it can again become non-zero. In our model the RG effects are negligible and $\overline{\theta}$ does not run very much. The leading contribution to $\overline{\theta}$ comes from higher dimensional operators such as

$$\delta\mathscr{L} \supset Y_u H Q u^c \frac{H H^\dagger}{M_{\mathrm{Pl}}^2} + Y_u H' Q' u'^c \frac{H' H'^\dagger}{M_{\mathrm{Pl}}^2}. \tag{2.5}$$

Using a chiral rotation, we see that this changes θ (θ') by $\sim H H^\dagger / M_{\mathrm{Pl}}^2$ ($H' H'^\dagger / M_{\mathrm{Pl}}^2$). When the two Higgs vevs become unequal, these operators lead to a non zero theta angle at low

energies

$$\overline{\theta} \sim \frac{h'^2 - h^2}{M_{\rm Pl}^2} \gtrsim 10^{-8} \tag{2.6}$$

for the range of h' vevs shown in Fig. 2. For $\mathcal{O}(1)$ Wilson coefficients for operators in Eq. 2.5, this is two orders of magnitude bigger than the current best limits from neutron [27] and mercury electric dipole moment searches [28, 29]. The remaining tuning of $\overline{\theta}$ can be alleviated further with larger representations (or more families) of the connector states $\psi^{(c)}$, which would lower the mirror Higgs vev h'.

2.2 Cosmology with a Mirror Sector

We conclude this section with a brief description of bounds on the reheat temperature of the universe. Because of the mirror baryon and electron number, the lightest stable particles of the other sector (their electrons, up quarks, and Dirac neutrinos) should never be in thermal equilibrium or they would overclose the universe.[5] Even in the most constraining situation, this only limits the reheat temperature to be beneath 10^{10} GeV, corresponding to the mass of the lightest charged mirror states. The glueballs and π' of QCD$'$ decay to SM hadrons before nucleosynthesis. A stronger constraint on the reheat temperature can come from overclosure due to stable ψ-baryons if their annihilation rate is too small. Alternatively, these states can play the role of dark matter if $\Lambda_{\rm QCD'}$ is low enough or if annihilation is otherwise enhanced, e.g., through a resonance.

The $\mathbb{Z}_2$ neutrinos are either extremely heavy (Majorana masses), ~ 100 GeV in mass (Dirac masses), or can even act as the right handed neutrinos through the higher dimensional operator [30]

$$\mathscr{L} \supset \frac{HLH'L'}{M_{\rm Pl}}. \tag{2.7}$$

Given bounds from over production of mirror electrons and quarks, the mirror neutrinos are never in thermal equilibrium. Dirac mirror neutrinos could be dark matter depending on how they are produced.

Even in the absence of mirror quarks and leptons, we cannot reheat above the scale $h' \gtrsim 10^{15}$ GeV as at that point thermal effects would stabilize the scalar field origin for both sectors. Both Higgses would live at the origin and the $\mathbb{Z}_2$ symmetry would be restored resulting in a $\mathbb{Z}_2$ symmetric universe.

3 Dimensional Transmutation from the Higgs quartic

In this section we discuss dimensional transmutation using the Higgs quartic. A second minimum in the Higgs potential is already generated in the SM for central values of the Higgs boson and top quark masses and the strong coupling α_s. This is the observation that the electroweak vacuum is metastable with a very long lifetime [4–6]. The expectation value

[5] This can be easily seen by the fact that they are parametrically heavier than the weak scale where the correct thermal relic density would be obtained.

of the Higgs field in the new minimum is far above the Planck scale where the SM is not valid [31]. However, in the presence of additional matter this minimum can move to sub-Planckian field values or disappear completely. The latter possibility has been considered by many authors and is arranged by adding new matter that alters the RG evolution of λ, see, e.g., Refs. [32–36]. In contrast, we will require that the SM vacuum is only metastable with the true minimum at sub-Planckian field values which can be studied using ordinary field theoretic methods. As we are considering the case where the Higgs is even more stable than in the SM, it is clear that the lifetime of the metastable vacua will be longer than the age of the universe.

3.1 Tree-Level Potential in the $\mathbb{Z}_2$-symmetric Standard Model

Our starting point is a $\mathbb{Z}_2$ or parity symmetric theory, as discussed in Sec. 1. The parity operation exchanges SM fields and gauge group for their $\mathbb{Z}_2$ partners, denoted by primed quantities. This symmetry ensures that the behavior of the effective potentials for the two Higgs states is the same at large field values. The tree-level $\mathbb{Z}_2$ symmetric scalar potential is

$$V_0 = -m_H^2(|H|^2 + |H'|^2) + \lambda(|H|^4 + |H'|^4) + \delta|H|^2|H'|^2, \tag{3.1}$$

with $H^{(\prime)}$ having the vacuum expectation value $h^{(\prime)}/\sqrt{2}$. We will consider the case where loop corrections to this potential are important. As a result, the Higgs obtains a second minimum at scales far above the weak scale but below the Planck scale. For simplicity we also set $\delta \ll g_1, g_2, y_t$ at a high scale so that its impact on the RG running of the quartic is negligible; this coupling will change due to RG evolution in the presence of matter charged under both copies of the gauge group, but at a very high loop order. This restriction allows us to consider the effective potentials of SM and SM$'$ separately in the following sections. When H' obtains an expectation value the tree-level Higgs mass is shifted by $\delta h'^2/2$, which can be large even if δ is small. This dynamical contribution to m_H^2 is subleading with respect to the usual naturalness problem and is dealt with by the "non-standard" solutions to the electroweak hierarchy discussed in the introduction.

3.2 Renormalization Group and the Effective Potential

Dimensional transmutation with the Higgs quartic λ happens at large field values. In order to reliably study the potential in this regime we use the renormalization group-improved potential, where the couplings are evaluated at the scale of the field value. We work in the two-loop approximation both for the potential and the RG evolution of the coupling constants. This amounts to a next-to-leading log resummation [37, 38].[6]

At high field values where the mass parameter can be neglected, the SM Higgs potential can be cast into the tree level-like expression [39]

$$V(h) \approx \frac{\lambda_{\rm eff}(h)}{4} h^4, \tag{3.2}$$

[6]Next-to-leading log accuracy is obtained already with the one loop potential improved by two loop beta functions.

where the effective quartic interaction $\lambda_{\rm eff}$ encodes the loop corrections to the potential

$$\lambda_{\rm eff}(h) = \lambda(\mu = h) + \frac{4}{h^4}\left(V_1(\mu = h) + V_2(\mu = h) + \dots\right), \tag{3.3}$$

and $V_1(\mu)$ and $V_2(\mu)$ are the one- and two-loop contributions to the effective potential. All couplings in Eq. 3.2 are evaluated at the scale $\mu = h$. In the one- and two-loop potentials above we include the contributions of W and Z bosons, the top quark, the Higgs and its Goldstone modes. The two-loop potential has been evaluated in the SM [40] and in general theories [41] in the Landau gauge. We validated our implementation against the publicly available code `SMH` [42]. The evaluation of the general two-loop beta functions and anomalous dimensions of Refs. [43–46] has been automated in Refs. [47, 48]. Explicit expressions for the SM potential and beta functions can found in, e.g., Ref. [5].

The potential is renormalized in $\overline{\rm MS}$ at $\mu = M_t$, where M_t is the top quark pole mass. The corresponding $\overline{\rm MS}$ SM couplings at this scale are given in Ref. [5] in terms of observables, including M_t itself. In Fig. 3 we show the effective quartic coupling as a function of h for central values of SM parameters as the dashed line. The blue band corresponds to varying M_t within its 1σ uncertainty. Note that at large field values $\lambda_{\rm eff} < 0$ corresponding to a potential that is unbounded from below up to the Planck scale.

As discussed in Sec. 2.1, our example solution to the strong CP problem requires the addition of massless bifundamental quarks transforming as $(\mathbf{3}, \overline{\mathbf{3}})$ of $SU(3)_C \times SU(3)_{C'}$, see Fig. 1. These new states do not couple to the Higgs even at the two loop level, so for fixed RG scale μ the two-loop potential is exactly the same as in the SM. The potential is modified once we implement RG improvement and set $\mu = h$. The bifundamentals change the RG running of the QCD gauge coupling g_3 and the top quark Yukawa y_t:

$$\Delta\beta_{g_3} = \frac{1}{(4\pi)^2}\left(\frac{2}{3}N_{c'}g_3^3\right) + \frac{1}{(4\pi)^4}\left(\frac{38}{3}N_{c'}g_3^5\right), \tag{3.4}$$

$$\Delta\beta_{y_t} = \frac{1}{(4\pi)^4}\left(\frac{40}{9}N_{c'}g_3^4 y_t\right), \tag{3.5}$$

where $N_{c'} = 3$ is number of colors in $SU(3)_{C'}$. As we evolve the coupling constants of the SM into the UV, these additional fermions slow the running of g_3; as a result y_t runs faster toward zero due the larger g_3. The net effect is that the negative contribution of y_t to the Higgs quartic λ is reduced and it can run positive before the Planck scale. Note that this formally occurs at 3 loops – it is only captured by the leading and next-to-leading log resummation implemented by the RG improvement of the potential. We demonstrate the effect of the bifundamentals with a mass scale of 100 TeV on $\lambda_{\rm eff}$ in Fig. 3 as the solid red line. As before, the band around the solid line corresponds to 1σ variations of M_t. Note that $\lambda_{\rm eff}$ runs positive at $h \sim 10^{16}$ GeV.

In the next section we study the extrema of the potential and determine confinement scale of QCD$'$.

3.3 Bifundamental Mass Scale

The scale at which the bifundamentals are integrated in or out is not a free parameter, but is rather fixed by the confinement scale of QCD$'$, $\Lambda_{\rm QCD'}$. The latter is determined by the

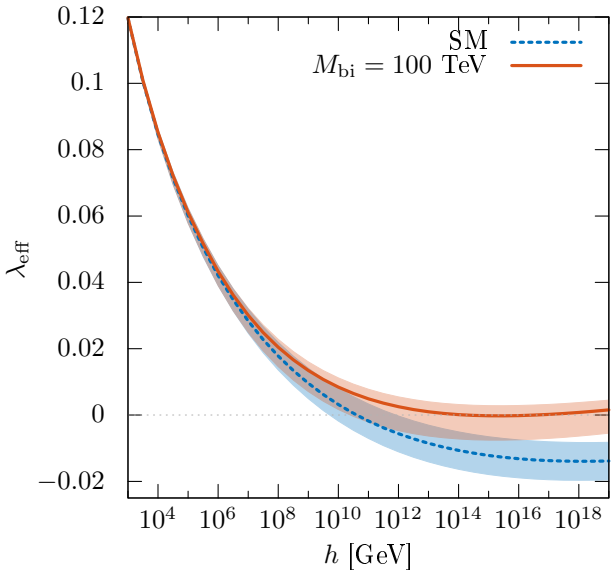

Figure 3: The effective quartic coupling as a function of the Higgs VEV for the SM field content and for a theory with additional $N_{c'} = 3$ new vector-like states charged under QCD that are integrated in at 100 TeV. The bands around each line correspond to varying M_t within 1σ.

masses of the $\mathbb{Z}_2$ quarks and the resulting RG evolution of g_3'.

Tree-level mirror quark masses only depend on the mirror Higgs vev h' and their Yukawa couplings. The location of extrema of Eq. 3.2 is obtained by solving

$$\lambda_{\rm eff}(h') + \frac{1}{4}\beta_{\lambda_{\rm eff}}(h') = 0, \tag{3.6}$$

where $\beta_{\lambda_{\rm eff}} = d\lambda_{\rm eff}/d\ln h'$. Note that potential, and therefore $\lambda_{\rm eff}$ are gauge-dependent quantities. The vev h' inherits this gauge dependence and is therefore not physical – see, e.g., Refs. [31, 49, 50] and references therein. Gauge invariant quantities can be obtained from pole masses [51]. The Higgs expectation value shown in Fig. 2 is computed using the physical W mass in the new minimum: $h_{\rm min} = 2m_W/g$. The Landau gauge self-energy needed for this is available in Ref. [52]. In Fig. 2 we see that the Higgs expectation values can be large and one might worry that the following results can be significantly altered by Planck-suppressed operators in the potential. We study these potential deformations in Appendix B and find that they do not change the main results of this section.

Once the mirror quark masses have been determined we run the QCD$'$ coupling g_3' from the scale of the vev into the IR using the QCD beta function in the one, two, three or four loop approximation [53]. The scale at which the coupling becomes non-perturbative, $g_3' \sim 4\pi$, defines the confinement scale $\Lambda_{\rm QCD'}$. As discussed in Sec. 2.1, in the IR QCD$'$ is a theory containing three massless flavors (the bifundamental quarks $\psi^{(c)}$), so its spectrum after confinement resembles low energy QCD. In particular, the physical scale of low energy

QCD$'$ corresponds to the mass of the lowest lying non-Goldstone meson – the ρ'. We determine the ρ' mass by

$$\frac{m_{\rho'}}{m_\rho} = \frac{\Lambda^{(l)}_{\mathrm{QCD}'}}{\Lambda^{(l)}_{\mathrm{QCD}}}, \tag{3.7}$$

where $m_\rho = 0.77$ GeV and Λ_{QCD} is the QCD confinement scale computed analogously to $\Lambda_{\mathrm{QCD}'}$. The superscript l indicates that the ratio of scales depends on the loop order of the beta function used. As in QCD, the lightest states are the Goldstone boson pions π' whose mass is determined by the explicit breaking of the global $SU(3)_L \times SU(3)_R$ through the gauging of QCD (see Sec. 2.1 and Ref. [13])

$$m^2_{\pi'} \approx \frac{9\alpha_s(m_{\pi'})}{4\pi} m^2_{\rho'}. \tag{3.8}$$

The dynamical scale $m_{\rho'}$ roughly determines where the bifundamental states are integrated into the running of our α_s and the strongly coupled physics is integrated out. Thus it has an important effect on the running of the Higgs quartic λ. Evolution through the strongly-coupled threshold of QCD$'$ can be done using dispersion relation methods. This problem is analogous to the running of α through the QCD confinement regime. In the SM the hadronic contribution to $\alpha(M_Z) - \alpha(0)$ is related to a measured cross-section using the optical theorem. We use the knowledge of low energy QCD to construct equivalent quantities in QCD$'$ and evaluate $\alpha_s(\mu \gtrsim m_{\rho'}) - \alpha_s(\mu \lesssim m_{\rho'})$. Below and above $\sim m_{\rho'}$, α_s is evolved using the usual perturbative beta functions. The discontinuity takes into account the neglected RG effects of the π' and ρ'. This procedure is described in detail in Appendix A.

The confinement scale of QCD$'$, $\Lambda_{\mathrm{QCD}'}$, determines when the the bifundamental states appear in the RGEs, which, in turn sets h', the vev in mirror sector. The latter feeds back into $\Lambda_{\mathrm{QCD}'}$ through the mirror quark masses. Thus $\Lambda_{\mathrm{QCD}'}$, or equivalently, $m_{\rho'}$, must be determined recursively. A self-consistent solution for $m_{\rho'}$ does not always exist. To understand this, consider fixing M_t and integrating in the bifundamentals at a scale $\mu = M_{\mathrm{bi}}$. Above some maximum value of $M_{\mathrm{bi}} = M^{\mathrm{max}}_{\mathrm{bi}}$, the RG effect of the bifundamentals is not enough to stabilize the potential at sub-Planckian field values, that is $V'(M_{\mathrm{Pl}}) < 0$. Similarly, below a minimum value of $M_{\mathrm{bi}} = M^{\mathrm{min}}_{\mathrm{bi}}$ the stabilizing effect of the bifundamentals is too large and the electroweak minimum is absolutely stable, i.e., Eq. 3.6 is never satisfied. The dependence of $M^{\mathrm{min}}_{\mathrm{bi}}$ and $M^{\mathrm{max}}_{\mathrm{bi}}$ on M_t is shown in Fig. 4 as the upper and lower dashed lines, respectively. For intermediate M_{bi}, a second, non-electroweak minimum exists with a sub-Planckian vev, allowing us to search for a solution to

$$M_{\mathrm{bi}} \sim m_{\rho'}(M_{\mathrm{bi}}), \tag{3.9}$$

where $m_{\rho'}$ is determined as described above and the argument indicates that it is a functional of M_{bi} through the RG equations and potential minimization. Solutions to this equation exist only in a narrow range of M_t, as shown in Fig. 4 by the solid black line. Above a maximum M^{max}_t, the bifundamental scale needed to stabilize the potential becomes lower than the minimum allowed value (the lower dashed line). In the other limit,

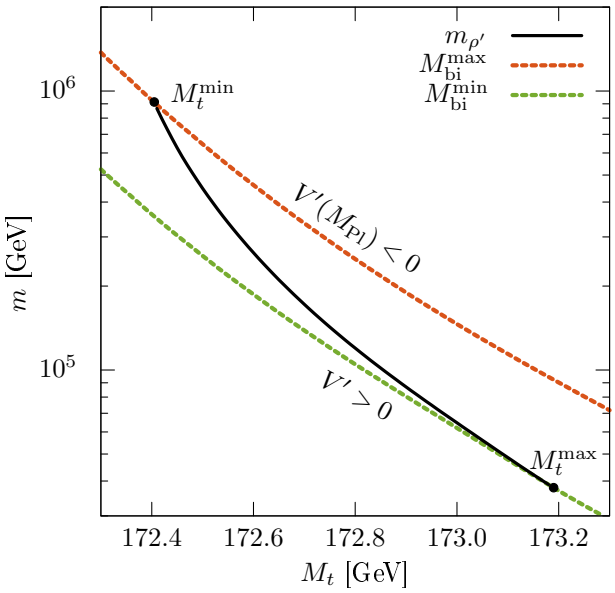

Figure 4: Minimum and maximum values of the bifundamental scale $M_{\rm bi}$ (dashed lines) as a function of the input top mass M_t. The solid line is the mass of ρ' determined self-consistently from the confinement scale of QCD$'$ as described in the text. Below $M_{\rm bi}^{\rm min}$ (lower dashed line) no minimum in the potential is generated by loop corrections. Above $M_{\rm bi}^{\rm max}$ (upper dashed line) the minimum occurs above $M_{\rm Pl}$.

as M_t is lowered the potential becomes more stable (due to smaller y_t) and the $m_{\rho'}$ needed to generate a new minimum increases, eventually crossing the maximum allowed value (upper dashed line) when $M_t = M_t^{\rm min}$.

We conclude this section by considering the sources of uncertainty in the physical outputs of this framework – the mass scale of the bifundamental states and range of "valid" M_t. The dominant sources of this uncertainty are related to the strongly-coupled regime of QCD$'$. First, the RG evolution through the strongly coupled regime of QCD$'$ depends on the precise low energy spectrum of that theory. While we constructed a reasonable model based on symmetry arguments (see Appendix A), a non-perturbative determination of the spectrum and the resulting threshold correction to α_s is desirable. This can be achieved, for example, with lattice simulations or with holographic methods [54]. We estimated the uncertainty associated with this calculation by varying the matching scale at which this threshold is applied, as described in Appendix A. The resulting uncertainty bands are shown in Fig. 2. This variation also shifts the valid range of M_t by ~ 0.5 GeV, which is not shown in the figure.

Second, our determination of $\Lambda_{\rm QCD'}$ relies on perturbative beta functions, leading to different values depending on loop order used. The variation with loop order is shown in the right plot of Fig. 2: the solid (dashed) line corresponds to the four (one) loop determination of $\Lambda_{\rm QCD'}$.

Another uncertainty is associated with matching at the electroweak scale and variation of $\alpha_s(M_Z)$ and M_h within their experimental error bars. In a full SM next-to-next-to-leading order (NNLO) computation (the current state-of-the-art) this amounts to an uncertainty of ~ 0.5 GeV on the critical value of M_t that leads to a stable electroweak minimum [6, 55]. We expect a somewhat larger uncertainty on the postdicted range of M_t with our approximations due to the absence of three-loop RGE. Beyond NNLO, the neglected higher-order terms in the effective potential and beta functions are expected to have a negligible effect [55]. Lastly, Planck suppressed operators can modify the shape of the potential at large field values. As long as the gauge invariant quantities associated with the vev are much smaller than $M_{\rm Pl}$, we expect these (unknown) effects to be unimportant [50]. Nevertheless, we consider the impact of these deformations in Appendix B, finding no qualitative changes to the main results of this section.

4 Conclusion

We have considered a solution to the hierarchy problem associated with a new scalar field. The new tree-level mass terms are related to the Standard Model Higgs mass by a discrete symmetry and are therefore protected from large corrections by the same mechanism that resolves the usual electroweak hierarchy problem. The new scalar obtains its mass and expectation value through dimensional transmutation of the Higgs quartic coupling, allowing these dimensionful quantities to be significantly different from the electroweak scale, while remaining technically natural. We illustrated this mechanism in the context of an η' solution to the strong CP problem, which employs a $\mathbb{Z}_2$ symmetry and new massless quarks to rotate away the QCD theta angle. The resulting model predicts scalar color octet states and determines their mass in terms of the Standard Model input parameters (and the representation of the new quarks).

The solution to the "wrong" hierarchy problem presented here, while extremely predictive, leaves open a few questions. First, what is the cosmological history of these solutions? Aside from the constraint that the reheating temperature is smaller than the scale at which parity or $\mathbb{Z}_2$ symmetry is restored, there is the question of how the universe ended up in the metastable state of one Higgs and in the true minimum of the other. It would be interesting to find a convincing reason for why this could be a generic occurrence.

It is also interesting to determine if there exist solutions to other problems of the SM which are testable in this framework. For example, one might utilize this effect to solve the doublet triplet splitting problem in Grand Unified Theories. Because the other scalar obtains a expectation value, one would need to enlarge $SU(3)_C$ to $SU(4)_C$ at high scales. Another use of this solution to the hierarchy problem is to use a $\mathbb{Z}_2$ version of the currently excluded Higgs as a flavon theory [56, 57]. Using the sum $h^2 + h'^2$ as the flavon puts the flavor scale at a very safe but very unobservable large value. This effect also fits well with Left-Right (LR) symmetric models as it avoids the need for additional bifundamental scalar fields (see e.g. Ref. [58]) leading to very predictive but also unobservable scenarios.

Of course the most interesting extension would be applying this solution to the SM Higgs boson. As in similar scenarios with Coleman-Weinberg electroweak symmetry break-

ing (see, e.g., Ref. [59]), this is difficult to achieve. First, the Coleman-Weinberg minimum has a Higgs mass parametrically smaller than its expectation value, something not seen with the SM Higgs. Second, the cubic and quartic Higgs self-interactions would deviate significantly from their SM values. Third, the potential minimization condition, Eq. 3.6, implies that at the radiatively-generated minimum the effective quartic has a positive beta function. For the SM Higgs boson the large top Yukawa drives this beta function negative at low energies, so new bosonic degrees of freedom at relatively low masses are required to make it positive [59].

In this paper, another small step was taken towards finding non-standard solutions to hierarchy problems. These mechanisms have not been thoroughly explored before and there may be many interesting solutions that are still undiscovered. In continuing along the direction of this work, it would be extremely interesting if one could dimensionally transmute the Higgs scale itself, from, e.g., the scale of the cosmological constant.

Acknowledgments

We thank Stephen Martin, Michael Peskin, Lance Dixon, Brian Shuve for helpful discussions and David Morrissey for feedback on the manuscript. N.B. is supported by DOE Contract DE-AC02-76SF00515. A.H. is supported by the DOE Grant DE-SC0012012 and NSF Grant 1316699.

A Integrating Through a Strongly Coupled Threshold

The RG evolution of the QCD coupling g_3 passes through the confinement scale of QCD$'$. Above this threshold the degrees of freedom contributing to the beta function are the free quarks and the bifundamentals, while below only the quarks contribute. In the intermediate region, the degrees of freedom associated with the bifundamentals are strongly coupled and consist of various mirror hadrons that carry QCD charge. A similar situation arises in the SM when we want to evaluate the the shift in electromagnetic coupling $\Delta\alpha$ between momentum scales q_0^2 and q^2, with QCD confinement occurring inside this range. This is done using the once-subtracted dispersion relation for the gauge boson self-energy $\Pi(q^2)$ [60]

$$\Delta\alpha = \Pi(q^2) - \Pi(q_0^2) = \frac{(q^2 - q_0^2)}{\pi} \int_{s_{\rm thr}}^{\infty} ds \frac{\Im\Pi(s + i\epsilon)}{(s - q_0^2)(s - q^2)}, \tag{A.1}$$

where $s_{\rm thr}$ is the beginning of the branch cut corresponding to on-shell intermediate states, e.g. pions, ρ's, etc. and $q_0^2 < s_{\rm thr}$, i.e. $\Im\Pi(q_0^2) = 0$. In our case the lightest intermediate states are the π'. Thus we take $s_{\rm thr} = 4m_{\pi'}^2$.

In order to evaluate the integrand in Eq. A.1 we consider the forward scattering amplitude $\bar{q}q \to \bar{q}q$. We can isolate the imaginary part of the gluon self-energy by considering only the processes that occur through an s-channel gluon exchange. There are others, such as box diagrams with two intermediate gluons, but these are higher order in g_3. Applying the optical theorem and summing over initial and final colors and spins we find

$$\Im\Pi(s) = -\left[\frac{N_c^2}{(N_c^2 - 1)T_F}\right]\left[\frac{s}{4\pi\alpha_s}\right]\sigma(\bar{q}q \to \text{hadrons}'), \tag{A.2}$$

where $N_c = 3$ and $T_F = 1/2$. In the non-perturbative regime we must use the measured $\sigma(e^+e^- \to \text{hadrons})$, suitably scaled to model $\sigma(\bar{q}q \to \text{hadrons}')$. Note, however, that the physical QCD spectrum *is* dictated by explicit breaking of chiral symmetry through non-zero quark masses. This splits various states that would be degenerate in QCD′. Thus a conservative approach is not to use the full $R(s)$ but only the contribution from $e^+e^- \to \pi^+\pi^-$ (corresponding to $\bar{q}q \to \pi'\pi'$ in QCD′), which dominates at low energies. At higher energies we switch to the perturbative cross-section, where is it a good description of the data. By restricting ourselves to the $\pi\pi$ final state in the non-perturbative regime, the group-theoretic factors can be easily accounted for. An analytical fit in terms masses of π and the vector mesons for $e^+e^- \to \pi^+\pi^-$ is given in Ref. [61]. We use this result by rescaling the parameters of the fit to account for different meson masses in QCD′.

Let us define a quantity $R'(s)$ that resembles the SM hadronic R function:

$$R'(s) = \kappa \frac{\sigma(\bar{q}q \to \pi'\pi')}{\sigma(\bar{q}q \to \bar{q}'q')} = -\frac{3\kappa}{\alpha_s T_F} \Im\Pi(s), \tag{A.3}$$

where

$$\sigma(\bar{q}q \to \bar{q}'q') = \left[\frac{(N_c^2-1)T_F^2}{N_c^2}\right] \frac{4\pi\alpha_s^2}{3s}, \tag{A.4}$$

and κ is a numerical factor to be fixed later. Using Eq. A.3 in Eq. A.1 we find

$$\Delta\alpha_s^{(\text{QCD}')} = \Pi(q^2) - \Pi(q_0^2) = -\frac{\alpha_s T_F (q^2 - q_0^2)}{3\pi\kappa} \int_{s_{\text{thr}}}^{\infty} ds \frac{R'(s)}{(s-q_0^2)(s-q^2)}, \tag{A.5}$$

where the superscript indicates that this is only the contribution of the QCD′ states - running of α_s due to SM quarks still needs to be included. This is identical to the usual formula for $\Delta\alpha_{\text{had}}$ [60] for $q_0^2 = 0$, and $\kappa,\ T_F \to 1$.

The integral in Eq. A.5 is performed numerically using a data-driven model for $R'(s)$. We use the observed R to model R' in the non-perturbative regime. We take the analytic model of the $\pi\pi$ contribution to R from Ref. [61] and replace all dimensionful parameters by their QCD′ analogues and find

$$R \approx \frac{\sigma(e^+e^- \to \pi^+\pi^-)}{\sigma(e^+e^- \to \mu^+\mu^-)} = \frac{T_F}{C_A} \frac{\sigma(\bar{q}q \to \pi'\pi')}{\sigma(\bar{q}q \to \bar{q}'q')} = R', \tag{A.6}$$

where $C_A = N_c$. This defines

$$\kappa = \frac{T_F}{C_A}. \tag{A.7}$$

Equation A.6 must be used in the non-perturbative regime. We switch to the perturbative result for annihilation into the massless bifundamentals

$$R'(s) \approx \kappa N_c, \tag{A.8}$$

when the perturbative and non-perturbative results become equal above $s \gtrsim (m_{\rho'})^2$. The threshold correction of Eq. A.5 is applied between $q_0^2 \approx (m_{\pi'})^2$ and $q^2 \approx (3m_{\rho'})^2$, above which normal perturbative RG evolution is resumed. The values of q_0^2 and q^2 are chosen to lie well below and well above the hadronic resonances, respectively. The uncertainty bands in Fig. 2 were estimated by varying q from $3m_{\rho'}$ to $6m_{\rho'}$.

B Higher Dimensional Operators in the Scalar Potential

Stability constraints in the SM are sensitive to higher-dimensional operators in the potential, even if they are suppressed by $M_{\rm Pl}$ [31]. They can also drastically alter the lifetime of metastable vacua [62, 63]. In this Appendix we investigate the sensitivity of our results to the presence of operators of the form $\pm|H|^6/M_{\rm Pl}^2$. For $h \sim 10^{17}$ GeV these terms are comparable in magnitude to the other terms in the effective potential; comparing this with Fig. 2 we see that such operators can have a significant effect for some values of M_t.

First, we consider the operators $+|H|^6/M_{\rm Pl}^2$. This term stabilizes the potential at large field values. Even without additional matter the Higgs potential develops a minimum with expectation value $h_{\rm min}^{(\rm SM)} \sim 10^{18}$ GeV. This vev can be used to define the maximum bifundamental mass scale $M_{\rm bi}^{\rm max}$, since the bifundamental states give an additional stabilizing effect leading to $h_{\rm min} < h_{\rm min}^{(\rm SM)}$. The minimum scale $M_{\rm bi}^{\rm min}$ is defined as in Sec. 3.3. With these bounds in hand, we solve the self-consistency equation, Eq. 3.9, for $m_{\rho'}$. The resulting solution is shown in the left plot of Fig. 5. As before the solution only exists in a small range of M_t.

Next we consider $-|H|^6/M_{\rm Pl}^2$. Since this destabilizes the potential, it must be compensated by even higher dimensional operators like $|H|^8/M_{\rm Pl}^2$. Interestingly, even in this case the bifundamental states can lead to a new minimum in the potential. The bounds on the bifundamental mass scale arise from considerations similar to those in Sec. 3.3. Above a maximum value $M_{\rm bi}^{\rm max}$, no second minimum exists. Below the minimum $M_{\rm bi}^{\rm min}$ the potential develops an instability, but only due to the higher dimensional operator and not due to y_t. This gives rise to very tight band of bifundamental mass scales in which a solution to Eq. 3.9 may exist. This is shown in the right plot of Fig. 5.

In both cases above, the additional Planck-suppressed operators reduce the range of M_t for which a self-consistent solution for $m_{\rho'}$ exists. Comparing Figs. 4 and 5 we find that the resulting values of $m_{\rho'}$ are not very different from the case with no higher-dimensional operators. Thus we conclude that these deformations of the potential do not affect the qualitative features of the mechanism presented in Sec. 3.

References

[1] P. W. Graham, D. E. Kaplan, and S. Rajendran, "Cosmological Relaxation of the Electroweak Scale," *Phys. Rev. Lett.* **115** (2015) no. 22, 221801, arXiv:1504.07551 [hep-ph].

[2] N. Arkani-Hamed, T. Cohen, R. D'Agnolo, A. Hook, H. D. Kim, and D. Pinner, "NNaturalness," *To appear* .

[3] S. R. Coleman and E. J. Weinberg, "Radiative Corrections as the Origin of Spontaneous Symmetry Breaking," *Phys. Rev.* **D7** (1973) 1888–1910.

[4] G. Degrassi, S. Di Vita, J. Elias-Miro, J. R. Espinosa, G. F. Giudice, G. Isidori, and A. Strumia, "Higgs mass and vacuum stability in the Standard Model at NNLO," *JHEP* **08** (2012) 098, arXiv:1205.6497 [hep-ph].

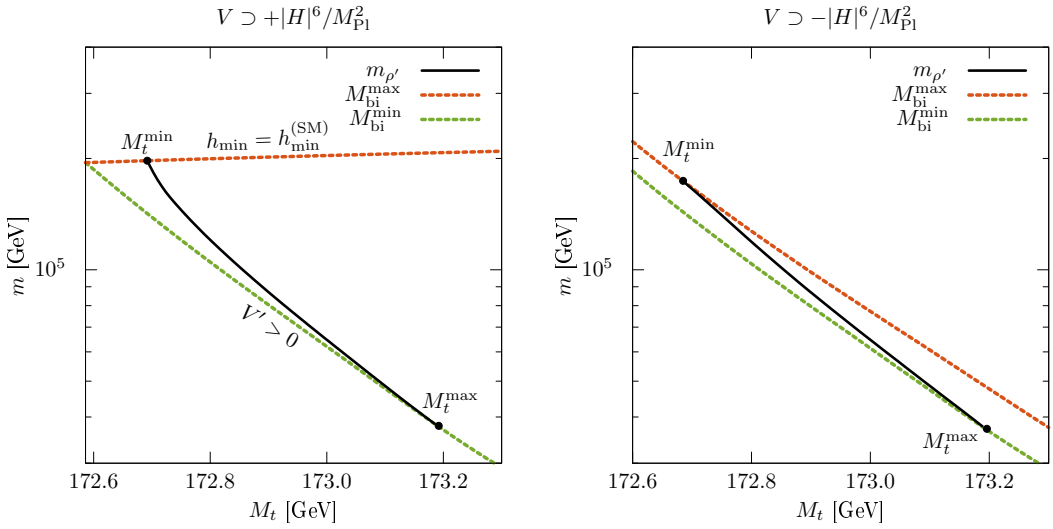

Figure 5: Prediction of $m_{\rho'}$ and viable range of M_t in the presence of Planck-suppressed operators $\pm|H|^6/M_{\rm Pl}^2$. The minimum and maximum values of the bifundamental scale are defined in the text.

[5] D. Buttazzo, G. Degrassi, P. P. Giardino, G. F. Giudice, F. Sala, A. Salvio, and A. Strumia, "Investigating the near-criticality of the Higgs boson," *JHEP* **12** (2013) 089, arXiv:1307.3536 [hep-ph].

[6] A. V. Bednyakov, B. A. Kniehl, A. F. Pikelner, and O. L. Veretin, "Stability of the Electroweak Vacuum: Gauge Independence and Advanced Precision," *Phys. Rev. Lett.* **115** (2015) no. 20, 201802, arXiv:1507.08833 [hep-ph].

[7] M. B. Einhorn and D. R. T. Jones, "The Effective potential, the renormalisation group and vacuum stability," *JHEP* **04** (2007) 051, arXiv:hep-ph/0702295 [HEP-PH].

[8] A. Salvio and A. Strumia, "Agravity," *JHEP* **06** (2014) 080, arXiv:1403.4226 [hep-ph].

[9] L. B. Okun, "Mirror particles and mirror matter: 50 years of speculations and search," *Phys. Usp.* **50** (2007) 380–389, arXiv:hep-ph/0606202 [hep-ph].

[10] Z. Chacko, H.-S. Goh, and R. Harnik, "The Twin Higgs: Natural electroweak breaking from mirror symmetry," *Phys. Rev. Lett.* **96** (2006) 231802, arXiv:hep-ph/0506256 [hep-ph].

[11] H. An, S.-L. Chen, R. N. Mohapatra, and Y. Zhang, "Leptogenesis as a Common Origin for Matter and Dark Matter," *JHEP* **03** (2010) 124, arXiv:0911.4463 [hep-ph].

[12] Z. Berezhiani, L. Gianfagna, and M. Giannotti, "Strong CP problem and mirror world: The Weinberg-Wilczek axion revisited," *Phys. Lett.* **B500** (2001) 286–296, arXiv:hep-ph/0009290 [hep-ph].

[13] A. Hook, "Anomalous solutions to the strong CP problem," *Phys. Rev. Lett.* **114** (2015) no. 14, 141801, arXiv:1411.3325 [hep-ph].

[14] R. T. D'Agnolo and A. Hook, "Finding the Strong CP problem at the LHC," arXiv:1507.00336 [hep-ph].

[15] R. Foot, "Mirror dark matter: Cosmology, galaxy structure and direct detection," *Int. J. Mod. Phys.* **A29** (2014) 1430013, arXiv:1401.3965 [astro-ph.CO].

[16] A. Albaid, M. Dine, and P. Draper, "Strong CP and SUZ_2," *JHEP* **12** (2015) 046, arXiv:1510.03392 [hep-ph].

[17] M. Dine and P. Draper, "Challenges for the Nelson-Barr Mechanism," *JHEP* **08** (2015) 132, arXiv:1506.05433 [hep-ph].

[18] J. R. Ellis and M. K. Gaillard, "Strong and Weak CP Violation," *Nucl.Phys.* **B150** (1979) 141.

[19] I. B. Khriplovich and A. I. Vainshtein, "Infinite renormalization of Theta term and Jarlskog invariant for CP violation," *Nucl. Phys.* **B414** (1994) 27–32, arXiv:hep-ph/9308334 [hep-ph].

[20] **Particle Data Group** Collaboration, K. A. Olive *et al.*, "Review of Particle Physics," *Chin. Phys.* **C38** (2014) 090001.

[21] K. Fujii *et al.*, "Physics Case for the International Linear Collider," arXiv:1506.05992 [hep-ex].

[22] T. Han, I. Lewis, and Z. Liu, "Colored Resonant Signals at the LHC: Largest Rate and Simplest Topology," *JHEP* **12** (2010) 085, arXiv:1010.4309 [hep-ph].

[23] C.-Y. Chen, A. Freitas, T. Han, and K. S. M. Lee, "Heavy Color-Octet Particles at the LHC," *JHEP* **05** (2015) 135, arXiv:1410.8113 [hep-ph].

[24] G. Cacciapaglia, H. Cai, A. Deandrea, T. Flacke, S. J. Lee, and A. Parolini, "Composite scalars at the LHC: the Higgs, the Sextet and the Octet," *JHEP* **11** (2015) 201, arXiv:1507.02283 [hep-ph].

[25] N. Arkani-Hamed, T. Han, M. Mangano, and L.-T. Wang, "Physics Opportunities of a 100 TeV Proton-Proton Collider," arXiv:1511.06495 [hep-ph].

[26] M. Kamionkowski and J. March-Russell, "Planck scale physics and the Peccei-Quinn mechanism," *Phys. Lett.* **B282** (1992) 137–141, arXiv:hep-th/9202003 [hep-th].

[27] C. A. Baker *et al.*, "An Improved experimental limit on the electric dipole moment of the neutron," *Phys. Rev. Lett.* **97** (2006) 131801, arXiv:hep-ex/0602020 [hep-ex].

[28] W. C. Griffith, M. D. Swallows, T. H. Loftus, M. V. Romalis, B. R. Heckel, and E. N. Fortson, "Improved Limit on the Permanent Electric Dipole Moment of Hg-199," *Phys. Rev. Lett.* **102** (2009) 101601.

[29] J. Engel, M. J. Ramsey-Musolf, and U. van Kolck, "Electric Dipole Moments of Nucleons, Nuclei, and Atoms: The Standard Model and Beyond," *Prog. Part. Nucl. Phys.* **71** (2013) 21–74, arXiv:1303.2371 [nucl-th].

[30] E. K. Akhmedov, Z. G. Berezhiani, and G. Senjanovic, "Planck scale physics and neutrino masses," *Phys. Rev. Lett.* **69** (1992) 3013–3016, arXiv:hep-ph/9205230 [hep-ph].

[31] A. Andreassen, W. Frost, and M. D. Schwartz, "Consistent Use of the Standard Model Effective Potential," *Phys. Rev. Lett.* **113** (2014) no. 24, 241801, arXiv:1408.0292 [hep-ph].

[32] W. Chao, M. Gonderinger, and M. J. Ramsey-Musolf, "Higgs Vacuum Stability, Neutrino Mass, and Dark Matter," *Phys. Rev.* **D86** (2012) 113017, arXiv:1210.0491 [hep-ph].

[33] C.-S. Chen and Y. Tang, "Vacuum stability, neutrinos, and dark matter," *JHEP* **04** (2012) 019, arXiv:1202.5717 [hep-ph].

[34] J. Elias-Miro, J. R. Espinosa, G. F. Giudice, H. M. Lee, and A. Strumia, "Stabilization of the Electroweak Vacuum by a Scalar Threshold Effect," *JHEP* **06** (2012) 031, arXiv:1203.0237 [hep-ph].

[35] O. Lebedev, "On Stability of the Electroweak Vacuum and the Higgs Portal," *Eur. Phys. J.* **C72** (2012) 2058, arXiv:1203.0156 [hep-ph].

[36] J. R. Espinosa, "Implications of the top (and Higgs) mass for vacuum stability," in *8th International Workshop on Top Quark Physics (TOP2015) Ischia, NA, Italy, September 14-18, 2015*. 2015. arXiv:1512.01222 [hep-ph]. http://inspirehep.net/record/1407977/files/arXiv:1512.01222.pdf.

[37] B. M. Kastening, "Renormalization group improvement of the effective potential in massive phi**4 theory," *Phys. Lett.* **B283** (1992) 287–292.

[38] M. Bando, T. Kugo, N. Maekawa, and H. Nakano, "Improving the effective potential," *Phys. Lett.* **B301** (1993) 83–89, arXiv:hep-ph/9210228 [hep-ph].

[39] J. A. Casas, J. R. Espinosa, and M. Quiros, "Improved Higgs mass stability bound in the standard model and implications for supersymmetry," *Phys. Lett.* **B342** (1995) 171–179, arXiv:hep-ph/9409458 [hep-ph].

[40] C. Ford, I. Jack, and D. R. T. Jones, "The Standard model effective potential at two loops," *Nucl. Phys.* **B387** (1992) 373–390, arXiv:hep-ph/0111190 [hep-ph]. [Erratum: Nucl. Phys.B504,551(1997)].

[41] S. P. Martin, "Two loop effective potential for a general renormalizable theory and softly broken supersymmetry," *Phys. Rev.* **D65** (2002) 116003, arXiv:hep-ph/0111209 [hep-ph].

[42] S. P. Martin and D. G. Robertson, "Higgs boson mass in the Standard Model at two-loop order and beyond," *Phys. Rev.* **D90** (2014) no. 7, 073010, arXiv:1407.4336 [hep-ph].

[43] M. E. Machacek and M. T. Vaughn, "Two Loop Renormalization Group Equations in a General Quantum Field Theory. 1. Wave Function Renormalization," *Nucl.Phys.* **B222** (1983) 83.

[44] M. E. Machacek and M. T. Vaughn, "Two Loop Renormalization Group Equations in a General Quantum Field Theory. 2. Yukawa Couplings," *Nucl.Phys.* **B236** (1984) 221.

[45] M. E. Machacek and M. T. Vaughn, "Two Loop Renormalization Group Equations in a General Quantum Field Theory. 3. Scalar Quartic Couplings," *Nucl.Phys.* **B249** (1985) 70.

[46] M.-x. Luo, H.-w. Wang, and Y. Xiao, "Two loop renormalization group equations in general gauge field theories," *Phys.Rev.* **D67** (2003) 065019, arXiv:hep-ph/0211440 [hep-ph].

[47] F. Staub, "SARAH 4: A tool for (not only SUSY) model builders," *Comput.Phys.Commun.* **185** (2014) 1773–1790, arXiv:1309.7223 [hep-ph].

[48] F. Lyonnet, I. Schienbein, F. Staub, and A. Wingerter, "PyR@TE: Renormalization Group Equations for General Gauge Theories," *Comput. Phys. Commun.* **185** (2014) 1130–1152, arXiv:1309.7030 [hep-ph].

[49] H. H. Patel and M. J. Ramsey-Musolf, "Baryon Washout, Electroweak Phase Transition, and Perturbation Theory," *JHEP* **07** (2011) 029, arXiv:1101.4665 [hep-ph].

[50] A. Andreassen, W. Frost, and M. D. Schwartz, "Consistent Use of Effective Potentials," *Phys. Rev.* **D91** (2015) no. 1, 016009, arXiv:1408.0287 [hep-ph].

[51] R. Hempfling and B. A. Kniehl, "On the relation between the fermion pole mass and MS Yukawa coupling in the standard model," *Phys. Rev.* **D51** (1995) 1386–1394, arXiv:hep-ph/9408313 [hep-ph].

[52] S. P. Martin, "Pole mass of the W boson at two-loop order in the pure $\overline{MS}$ scheme," *Phys. Rev.* **D91** (2015) no. 11, 114003, arXiv:1503.03782 [hep-ph].

[53] T. van Ritbergen, J. A. M. Vermaseren, and S. A. Larin, "The Four loop beta function in quantum chromodynamics," *Phys. Lett.* **B400** (1997) 379–384, arXiv:hep-ph/9701390 [hep-ph].

[54] S. J. Brodsky, A. Deur, G. F. de Tramond, and H. G. Dosch, "Light-Front Holography and Superconformal Quantum Mechanics: A New Approach to Hadron Structure and Color Confinement," *Int. J. Mod. Phys. Conf. Ser.* **39** (2015) 1560081, arXiv:1510.01011 [hep-ph].

[55] G. Iacobellis and I. Masina, "Stationary configurations of the Standard Model Higgs potential: electroweak stability and rising inflection point," arXiv:1604.06046 [hep-ph].

[56] K. S. Babu and S. Nandi, "Natural fermion mass hierarchy and new signals for the Higgs boson," *Phys. Rev.* **D62** (2000) 033002, arXiv:hep-ph/9907213 [hep-ph].

[57] G. F. Giudice and O. Lebedev, "Higgs-dependent Yukawa couplings," *Phys. Lett.* **B665** (2008) 79–85, arXiv:0804.1753 [hep-ph].

[58] G. Senjanovic and R. N. Mohapatra, "Exact Left-Right Symmetry and Spontaneous Violation of Parity," *Phys. Rev.* **D12** (1975) 1502.

[59] C. T. Hill, "Is the Higgs Boson Associated with Coleman-Weinberg Dynamical Symmetry Breaking?," *Phys. Rev.* **D89** (2014) no. 7, 073003, arXiv:1401.4185 [hep-ph].

[60] **Working Group on Radiative Corrections and Monte Carlo Generators for Low Energies** Collaboration, S. Actis *et al.*, "Quest for precision in hadronic cross sections at low energy: Monte Carlo tools vs. experimental data," *Eur. Phys. J.* **C66** (2010) 585–686, arXiv:0912.0749 [hep-ph].

[61] **BaBar** Collaboration, J. P. Lees *et al.*, "Precise Measurement of the $e^+e^- \to \pi^+\pi^-(\gamma)$ Cross Section with the Initial-State Radiation Method at BABAR," *Phys. Rev.* **D86** (2012) 032013, arXiv:1205.2228 [hep-ex].

[62] V. Branchina and E. Messina, "Stability, Higgs Boson Mass and New Physics," *Phys. Rev. Lett.* **111** (2013) 241801, arXiv:1307.5193 [hep-ph].

[63] A. Andreassen, D. Farhi, W. Frost, and M. D. Schwartz, "Precision decay rate calculations in quantum field theory," arXiv:1604.06090 [hep-th].